Synthesis of $Co^{II}Co^{III}_{2-x}Al_xO_4-Al_2O_3$ Nanocomposites via Decomposition of $Co^{II}_{0.73}Co^{III}_{0.27}(OH)_{2.00}(NO_3)_{0.23}(CO_3)_{0.02}\cdot 0.5H_2O$ in a Sol−Gel-Derived γ-Al_2O_3 Matrix

J. T. Sampanthar and H. C. Zeng*

Department of Chemical and Environmental Engineering, Faculty of Engineering, and Chemical and Process Engineering Center, National University of Singapore, 10 Kent Ridge Crescent, Singapore 119260, Singapore

Received June 7, 2001. Revised Manuscript Received September 5, 2001

Nanocomposite materials of $Co^{II}Co^{III}_{2-x}Al_xO_4-Al_2O_3$ ($0 \le x < 1.63$) have been prepared from biphasic xerogels that contain the cobalt hydrotalcite-like compound $Co^{II}_{0.73}Co^{III}_{0.27}(OH)_{2.00}(NO_3)_{0.23}(CO_3)_{0.02}\cdot 0.5H_2O$ and sol−gel-derived Al_2O_3. With XRD/FTIR/XPS/DSC/TGA methods, an investigation has been carried out to understand the formation processes of the composites and chemical reactivity of the embedded cobalt hydrotalcite-like compound with alumina gel matrixes at various heating temperatures. It has been found that cubic spinels of Co_3O_4 and $Co^{II}Co^{III}_{2-x}Al_xO_4$ are generated sequentially inside alumina matrixes upon decomposition of the hydrotalcite-like compound in static air. The average spinel crystallite size is in the range of 9−13 nm at 350 °C to 31−38 nm at 800 °C, whereas the specific surface area of the composites is reduced gradually from 277−363 $m^2\ g^{-1}$ at 350 °C to 184−224 $m^2\ g^{-1}$ at 800 °C. On one hand, the catalytic effect of cobalt on combustion reactions of organics trapped within the amorphous alumina gel matrixes is elucidated by varying the cobalt content and synthesis conditions. On the other hand, the retardation effect of γ-Al_2O_3 matrixes on the growth of the crystallite is also revealed. It has been indicated that the content of aluminum (x) in $Co^{II}Co^{III}_{2-x}Al_xO_4-Al_2O_3$ is indeed a function of the heating temperature. After thermal decomposition of the cobalt hydrotalcite-like compound, the Co_3O_4 phase starts to form at a temperature as low as 200 °C and is fully developed at 350 °C. At 500−800 °C, the formed Co_3O_4 is converted to the $Co^{II}Co^{III}_{2-x}Al_xO_4$ phase due to the reaction between the included phase and alumina matrixes.

Introduction

In the past decade, the synthesis of hydrotalcite-like compounds has attracted considerable attention in layered materials research.[1−10] In typical hydrotalcite-like compounds, a divalent metal cation is centered in octahedral sites formed by six hydroxyl groups. These octahedrons then share their edges to form two-dimensionally infinite layers, which is similar to the sheetlike structure of brucite $Mg(OH)_2$.[1] The stacking of these 2D sheets via various chemical interactions leads to a 3D solid. If some of the divalent cations in the 2D sheets are substituted by trivalent cations, organic or inorganic anions will be intercalated into the intersheet space (or interlayer space) to compensate for extra charges introduced by the trivalent cations, which results in a hydrotalcite-like structure named after the natural hydrotalcite compound $Mg_6Al_2(OH)_{16}CO_3\cdot 4H_2O$.[1] Therefore, this class of compounds is also known as anionic clays, owing to the presence of anionic species in the interlayer space. Although they are less well-known, compared to cationic clays, the anionic clays have been used in preparing catalyst and ceramic precursors, and in tailor-making anion adsorbents, medicine stabilizers, and ion exchangers in recent years.[1−10]

Very recently, we have succeeded in synthesizing the mono-transition-metal hydrotalcite-like compound $Co^{II}_{0.73}Co^{III}_{0.27}(OH)_{2.00}(NO_3)_{0.23}(CO_3)_{0.02}\cdot 0.5H_2O$ using a dy-

* To whom correspondence should be addressed. Phone: +65 874 2896. Fax: +65 779 1936. E-mail: chezhc@nus.edu.sg.

(1) Cavani, F.; Trifiro, F.; Vaccari, A. *Catal. Today* **1991**, *11*, 173 and references therein.

(2) Reiche, W. T. *Solid State Ionics* **1986**, *22*, 133 and references therein.

(3) Faure, C.; Borthomieu, Y.; Delmas, C.; Fonsassier, M. *J. Power Sources* **1991**, *36*, 113.

(4) (a) Armor, J. N.; Braymer, T. A.; Farris, T. S.; Li, Y.; Petrocelli, F. P.; Weist, E. L.; Kannan, S.; Swamy, C. S. *Appl. Catal., B* **1996**, *7*, 397 and references therein. (b) Kannan, S.; Swamy, C. S. *J. Mater. Sci.* **1997**, *32*, 1623.

(5) Hermosin, M. C.; Pavlovic, J.; Ulibarri, M. A.; Cornejo, J. *Water Res.* **1996**, *30*, 171.

(6) Chisem, I. C.; Jones, W. *J. Mater. Chem.* **1994**, *4*, 1737.

(7) (a) d'Espinose de la Caillerie, J. B.; Kermarec, M.; Clause, O. *J. Am. Chem. Soc.* **1995**, *117*, 11471. (b) Merlen, E.; Gueroult, P.; d'Espinose de la Caillerie, J. B.; Rebours, B.; Bobin, C.; Clause, O. *Appl. Clay Sci.* **1995**, *10*, 45.

(8) (a) Hibino, T.; Tsunashima, A. *Chem. Mater.* **1997**, *9*, 2082. (b) Velu, S.; Suzuki, K.; Okazaki, M.; Osaki, T.; Tomura, S.; Ohashi, F. *Chem. Mater.* **1999**, *11*, 2163. (c) Ogawa, M.; Asai, S. *Chem. Mater.* **2000**, *12*, 3253. (d) Hou, X. Q.; Kirkpatrick, R. J. *Chem. Mater.* **2000**, *12*, 1890.

(9) (a) Fogg, A. M.; Rohl, A. L.; Parkinson, G. M.; O'Hare, D. *Chem. Mater.* **1999**, *11*, 1194. (b) Choy, J. H.; Kwak, S. Y.; Park, J. S.; Jeong, Y. J.; Portier, J. *J. Am. Chem. Soc.* **1999**, *121*, 1399. (c) Choy, J. H.; Kwak, S. Y.; Jeong, Y. J.; Park, J. S. *Angew. Chem., Int. Ed. Engl.* **2000**, *39*, 4042.

(10) Rives, V.; Ulibarri, M. A. *Coord. Chem. Rev.* **1999**, *181*, 61 and references therein.

10.1021/cm010553o CCC: $20.00
Published on Web 11/30/2001

namic oxidation method.[11] It has been observed that, due to the presence of trivalent cobalt, the above hydrotalcite-like compound can be decomposed into cubic spinel Co_3O_4, an important magnetic and catalytic material, at relatively low temperatures even at ambient conditions.[12] In addition to this inorganic synthesis, we have also prepared nanometer-sized alumina materials via an organometallic sol−gel route.[13] It has been recognized that the high-surface-area alumina can be utilized as a matrix material to incorporate active chemical components such as transition-metal oxide particles acting as a secondary phase, which has been proved to be feasible in our recent synthesis of metal oxide nanocomposites RuO_2–Al_2O_3 with the ruthenium metal weight content at 0.5−2.0%.[14]

In the present work, we will incorporate the hydrotalcite-like compound $Co^{II}_{0.73}Co^{III}_{0.27}(OH)_{2.00}(NO_3)_{0.23}(CO_3)_{0.02}\cdot 0.5H_2O$ into the sol−gel-derived alumina matrixes. There are two objectives in this investigation: (i) fabrication of $Co^{II}Co^{III}_{2-x}Al_xO_4$−$Al_2O_3$ ($x \geq 0$) nanocomposites (in which at least one phase must be on the nanometer scale) using the newly synthesized cobalt hydrotalcite-like compound, in view of its low decomposition temperature,[11,12] and (ii) investigation of the thermal decomposition of hydrotalcite-like compounds in a confined space, such as in alumina matrixes in the present case. The first objective is raised owing to the fundamental interest of this magnetic material system (p-type semiconductor quantum dots embedded in an insulating matrix), while the second is directed to the general material issues of a new application of the hydrotalcite-like compounds in fabricating nanostructured materials.[15] To the best of our knowledge, the present work would also serve as the first example of thermal decomposition of hydrotalcite-like compounds in a confined gel space, as most work reported in the literature is conducted for single-phase compounds.[1,10]

Experimental Section

Sample Preparation. The cobalt-containing hydrotalcite-like compound $Co^{II}_{0.73}Co^{III}_{0.27}(OH)_{2.00}(NO_3)_{0.23}(CO_3)_{0.02}\cdot 0.5H_2O$ was prepared using a method published previously.[7,11] A 20.0 mL portion of 1.0 M aqueous cobalt nitrate solution was added (using a dropping funnel with a rate of about 5 mL min^{-1}) into 100.0 mL of 0.5 M ammoniacal solution (at 35 °C) in a three-necked round-bottom flask within 4−5 min under a purified oxygen atmosphere (Soxal at a rate of 40 mL min^{-1}. The reaction mixture was stirred continuously at 35 °C for 24 h under the same oxygen flow (i.e., aging process). The precipitate formed from this synthesis ($Co^{II}_{0.73}Co^{III}_{0.27}(OH)_{2.00}(NO_3)_{0.23}(CO_3)_{0.02}\cdot 0.5H_2O$) was filtrated and dried with a vacuum pump at room temperature for 2 days. The final pH of the filtrate was 8.3−8.5. The above vacuum-dried cobalt hydrotalcite-like compound (called the "HT sample" hereafter) was crushed into a very fine powder and sieved through a mesh wire filter (aperture 180 μm). Therefore, the powdered HT sample, which will be further used as a secondary phase to the alumina matrix, has a particulate size smaller than 180 μm.

The solution for the Al_2O_3 xerogel matrix was prepared using the following method.[13] In a typical synthesis, 25.0 mL of aluminum tri-*sec*-butoxide ($Al(O\text{-}s\text{-}Bu)_3$ or ASB; ACROS, 97%; 25.0 mL is equivalent to 98 mmol) was transferred to a 100.0 mL volumetric flask and then made up to 100 mL by adding 2-propanol (*i*-PrOH; Fisher Scientific, >99.9%) under a nitrogen atmosphere inside a drybox. At the same time, 3.0 mL of chelating agent 2,4-pentanedione (acetylacetone, $C_5H_8O_2$, or acacH; Merck, >99.5%; 3.0 mL is equivalent to 29 mmol) was also transferred to a 25.0 mL volumetric flask and then made up to 25 mL by adding 2-propanol. The above two solutions (total solution volume 100.0 mL + 25.0 mL) were then mixed and stirred for 30 min under a nitrogen atmosphere, which was followed by a further agitation in laboratory air for 30 min.

To prepare the $Co^{II}Co^{III}_{2-x}Al_xO_4$−$Al_2O_3$ nanocomposites, a desired amount of the solid HT sample was added to 25.0 mL (i.e., 1/5) of the above ASB/acacH/*i*-PrOH solution with vigorous stirring for 2 h. By adding deionized water (1.0−3.0 mL, Table 1) dropwise to the solid−solution mixture, hydrolysis of acacH-modified ASB was then started. The hydrolyzing mixture was covered and stirred continuously until gelation occurred (it took place within 6−12 h depending on the water amount added), which was followed by a 2-day static aging at room temperature. The aged alumina xerogels, which encapsulate HT powders, were dried at 60 °C in an electric oven for 2 more days. These biphasic samples (HT particulates + alumina matrix) were calcined in static air at different temperatures (200, 350, 500, and 800 °C) for 4 h with a heating rate of 5 °C min^{-1}. The chemical composition and nomenclature for some of these biphasic samples and their calcined oxides (i.e., $Co^{II}Co^{III}_{2-x}Al_xO_4$−$Al_2O_3$ nanocomposites, where x is the amount of trivalent aluminum in the spinel, $0 \leq x < 1.63$), are detailed in Tables 1 and 2.

Table 1. Chemical Compositions and Nomenclature for the Precursor Samples Synthesized in This Work

sample[a]	HT content[b] (mmol)	H_2O content[b] (mL)	H_2O/ASB[b] (mole ratio)	Co/Al (mole ratio)
A1	0.87	1.0	3	0.044
A2	1.32	1.0	3	0.067
A3	1.73	1.0	3	0.088
A4	2.17	1.0	3	0.111
A5	2.60	1.0	3	0.133
A3-1	1.73	0.5	1.5	0.088
A3-2	1.73	1.5	4	0.088
A3-3	1.73	2.0	6	0.088
A3-4	1.73	2.5	7	0.088
A3-5	1.73	3.0	9	0.088

[a] In all these samples, 19.6 mmol of ASB, 5.8 mmol of acacH, and 252 mmol of *i*-PrOH were used in the preparation. [b] The variable parameters in the synthesis are the HT content and water content, as indicated in the above table (see also the Experimental Section).

Table 2. Calculated Crystallite Sizes (nm) for the As-Prepared Samples and Their Heat-Treated Oxide Forms (i.e., $Co^{II}Co^{III}_{2-x}Al_xO_4$−$Al_2O_3$ Nanocomposites) at Different Temperatures

sample	25 or 60 °C[a]	350 °C[b]	500 °C[b]	800 °C[b]
HT	8.5	14.0		62.4
A1	8.4	11.6	16.1	36.9
A2	10.2	10.7	19.2	32.6
A3	10.7	12.5	15.1	31.0
A4	10.7	9.3	14.0	37.8
A5	10.2	12.1	14.1	35.0

[a] Crystallite sizes of the hydrotalcite-like phase in the as-prepared HT and biphasic xerogels after drying (see the Experimental Section and Figure 1); the (003) peaks were used in these calculations. [b] Crystallite sizes of the spinel phase in the decomposed HT or biphasic xerogels after various heat treatments (see the Experimental Section) in static air; the (311) peaks were used in these calculations.

Characterization Techniques. *XRD Measurement.* Crystallographic information on the samples was investigated by powder X-ray diffraction (XRD). Diffraction patterns of inten-

(11) Xu, Z. P.; Zeng, H. C. *Chem. Mater.* **2000**, *12*, 3459.
(12) Zeng, H. C.; Lim, Y. Y. *J. Mater. Res.* **2000**, *15*, 1250.
(13) Ji, L.; Lin, J.; Tan, K. L.; Zeng, H. C. *Chem. Mater.* **2000**, *12*, 931.
(14) Ji, L.; Lin, J.; Zeng, H. C. *Chem. Mater.* **2001**, *13*, 2403.
(15) Xu, Z. P.; Zeng, H. C. *J. Phys. Chem. B* **2000**, *104*, 10206.

sity versus 2θ were recorded with a Shimadzu XRD-6000 X-ray diffractometer using Cu Kα radiation ($\lambda = 1.5406$ Å) from 8° to 70° at a scanning speed of 2 deg min^{-1}. The *d* spacings of the as-prepared $Co^{II}_{0.73}Co^{III}_{0.27}(OH)_{2.00}(NO_3)_{0.23}(CO_3)_{0.02}\cdot 0.5H_2O$ and its calcined samples ($Co^{II}Co^{III}_{2-x}Al_xO_4-Al_2O_3$) were determined from the diffraction peaks/positions with structural analysis software, and the average crystallite sizes of the samples were estimated using the Debye−Scherrer formula from the full width at half-maximum (fwhm) of some intense peaks (Table 2).

FTIR Measurement. Chemical bonding information on metal−oxygen, hydroxyl, and other functional groups (such as nitrate anions and the acac group) were investigated with Fourier transform infrared spectroscopy (FTIR; Shimadzu FTIR-8101) using the potassium bromide (KBr) pellet technique. The FTIR spectrum background was corrected using a freshly prepared pure KBr pellet. Each FTIR spectrum was collected after 40 scans with a resolution of 2 cm^{-1}.

DSC/TGA Measurement. A differential scanning calorimetry (DSC; Netzsch DSC200) study was conducted to investigate thermal decomposition behaviors of the as-prepared HT and biphasic samples. DSC measurements were carried out from 30 to 400 °C at a scanning rate of 2 °C min^{-1} under an O_2 atmosphere and 10 °C min^{-1} under N_2. In both cases, the gas flow rate was kept at 15 mL min^{-1}. In thermogravimetric analysis (TGA; Shimadzu TGA-50), the furnace temperature was heated from room temperature to 900 °C at a rate of 2 °C min^{-1} with an air stream at 50 mL min^{-1}.

BET/BJH Measurement. Full adsorption−desorption isotherms of nitrogen at −195.8 °C on all calcined samples were measured at various partial pressures in a Quantachrome NOVA-3000 apparatus. Specific surface areas (S_{BET}) and pore-size distributions (PSDs) were determined using the Brunauer−Emmett−Teller (BET) method and Barret−Joyner−Hallenda (BJH) method, respectively.[16a] S_{BET} values were obtained from seven adsorption data points in the relative pressure (P/P^o) range 0.05−0.35 with the BET formalism, whereas the PSDs were derived from the desorption isotherms.[16a] Before the BET/BJH measurements, the samples were degassed for 3 h at a temperature slightly below that used in calcination or below 350 °C in general.

XPS Measurement. An X-ray photoelectron spectroscopy (XPS) investigation was conducted on an AXIS-Hsi spectrometer (Kratos Analytical) using a monochromated Al Kα X-ray source (1486.6 eV) at a constant analyzer pass energy of 20.0 eV. All binding energies (BEs) were referenced to the C 1s peak arising from adventitious carbon (BE = 284.5 eV). Prior to the peak deconvolution, X-ray satellites and the inelastic background (linear type) were subtracted for all spectra, and the curve fitting was then carried out using a least-squares fitting program.

Results and Discussion

Formation of Biphasic Xerogels. Figure 1 shows a series of XRD patterns of the HT-included biphasic xerogels (A1−A5, Table 1), together with those of the pure-phase HT compound and blank alumina gel matrix. The chemical and structural analysis for the included hydrotalcite-like compound $Co^{II}_{0.73}Co^{III}_{0.27}(OH)_{2.00}(NO_3)_{0.23}(CO_3)_{0.02}\cdot 0.5H_2O$ (HT) has been reported in detail in our previous publications.[7,11] In this work, all diffraction features of the hydrotalcite-like phase, such as (003), (006), (009), and (012) peaks, are well retained in samples A1−A5, while the amorphous nature of the alumina gel matrix is indicated as the background in the patterns. FTIR spectra for the as-prepared A1−A5 samples are displayed in Figure 2. Typical IR absorptions of aluminum acetylacetonate linkages can be observed over the wavenumber range 1900−900 cm^{-1} (ν(C−O), ν(C−C), etc.),[16b−e] which indicates the chelating agent acetylacetonate is still confined in the alumina gel matrix.[13] The broad absorptions below 900 cm^{-1} correspond to both the Al−O−Al network formed after hydrolysis and Co−O−Co in brucite-like sheets of the included HT phase. Some very weak bands appearing at 3000−2900 cm^{-1} are assigned

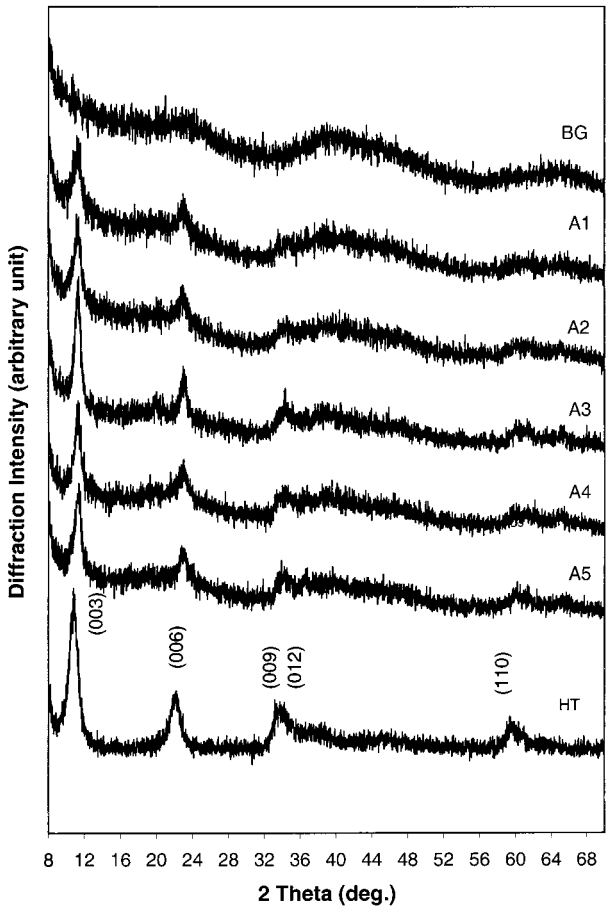

Figure 1. XRD patterns of the as-prepared hydrotalcite-like compound HT, the HT-included biphasic gel samples A1−A5, and the alumina BG.

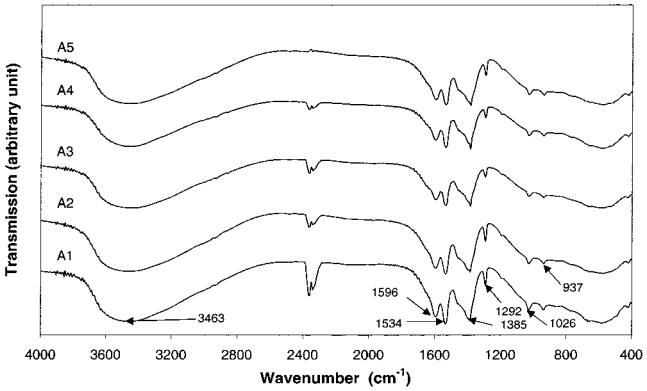

Figure 2. FTIR spectra of the HT-included biphasic gel samples A1−A5.

(16) (a) Sing, K. S. W.; Everett, D. H.; Haul, R. A. W.; Moscou, L.; Pierotti, R. A.; Rouquerol, J.; Siemieniewska, T. *Pure Appl. Chem.* **1985**, *57*, 603. (b) Guertin, D. L.; Wiberley, S. E.; Bauer, W. H.; Goldenson, J. *J. Phys. Chem.* **1956**, *60*, 1018. (c) Nakamoto, K. *Infrared Spectra of Inorganic and Coordination Compounds*; John Wiley and Sons: New York, 1962; p 216. (d) Nakamoto, K. *Infrared and Raman Spectra of Inorganic and Coordination Compounds*; John Wiley and Sons: New York, 1986; p 259. (e) Leaustic, A.; Babonneau, F.; Livage, J. *Chem. Mater.* **1989**, *1*, 240.

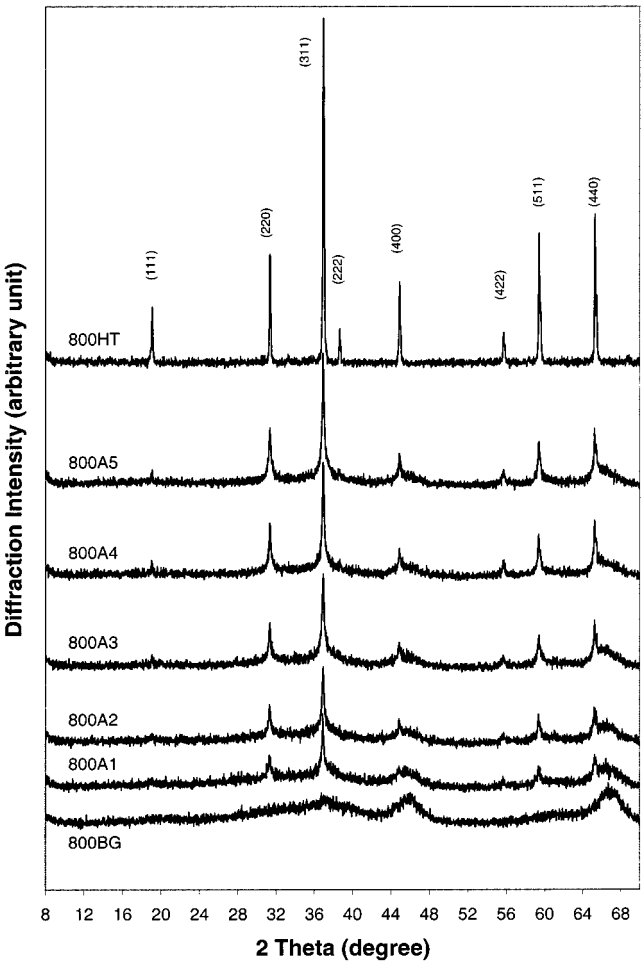

Figure 3. XRD patterns of the alumina BG, the hydrotalcite-like compound HT, and the HT-included biphasic gel samples A1−A5 heated at 800 °C. The prefix number 800 of the samples indicates a heating temperature of 800 °C (in static air, 4 h).

to the stretching vibration of C−H bonds in the acac groups.[17,18] A broad band centered at 3463 cm^{-1} corresponds to residual O−H groups of the synthesized products occluded within the alumina gel and planar O−H groups of the HT sample.[8,19] In good agreement with the HT inclusion, nitrate anions intercalated in the interlayer space of the HT compound can be clearly observed at 1385 cm^{-1}, which belongs to the ν_3 vibrational mode, with D_{3h} symmetry of the anions.[8,11] The absorption band over 2300−2500 cm^{-1} (also in Figure 5) is due to instrumental detection of atmospheric CO_2.

The above XRD/FTIR observations confirm the biphasic nature of the precursor materials. In particular, it can be concluded that there are no direct chemical reactions between the HT compound (secondary phase) and the matrix alumina at the low drying temperatures, as each phase still largely preserves its primitive form.

Generation of Nanocomposites. When the above biphasic samples are heat-treated at 800 °C in static air, $Co^{II}Co^{III}_{2-x}Al_xO_4-Al_2O_3$ nanocomposites result. As reported in Figure 3, cubic spinel phases of Co_3O_4 ($x = 0$) and/or $Co^{II}Co^{III}_{2-x}Al_xO_4$ ($0 < x < 1.63$) can be observed

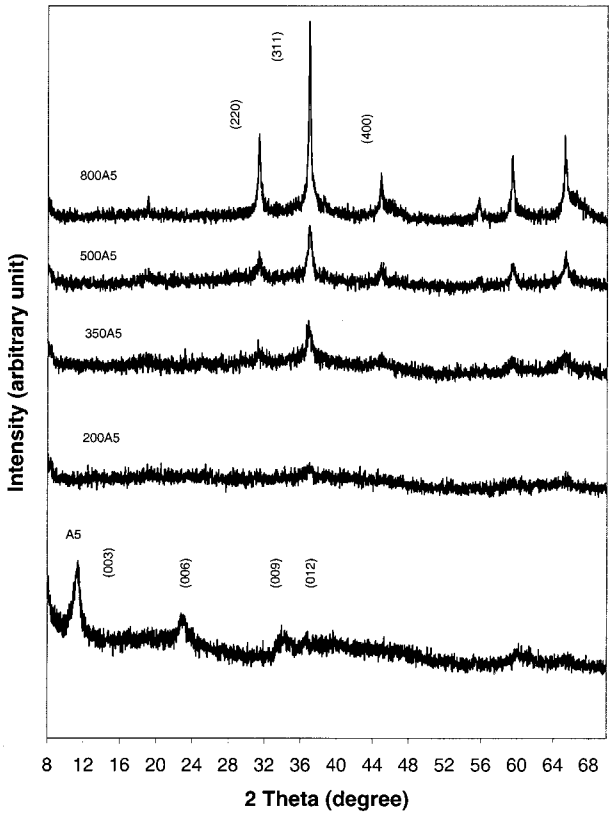

Figure 4. XRD patterns of the HT-included biphasic gel sample A5 heated at different temperatures. The prefix number of the samples indicates the heating temperature (°C) (in static air, 4 h).

on the background diffraction patterns of the γ-Al_2O_3 matrix, which also belongs to a cubic phase.[20] It is noted that the intensities of the spinel diffraction patterns increase with the content of the hydrotalcite-like compound introduced into the biphasic gels, whereas the diffraction patterns of γ-Al_2O_3 in all heated samples are the same because it is a predominant species. Since the estimated crystallite size for the γ-Al_2O_3 matrix is about 2−3 nm,[14] the resultant $Co^{II}Co^{III}_{2-x}Al_xO_4-Al_2O_3$ can indeed be called nanocomposites.

Figure 4 gives a set of XRD patterns for a representative biphasic sample (A5, with the highest HT content in the gel) after thermal treatment at different temperatures. Under an oxidative atmosphere, the included HT phase readily decomposes at a temperature as low as 200 °C. At 350 °C, the Co_3O_4 (and/or $Co^{II}Co^{III}_{2-x}Al_xO_4$) phase has been formed, with all characteristic diffraction peaks of the cubic spinel phase detected.[20] At higher temperatures, the spinel phase patterns become more intense and the diffraction peaks reduce their widths. An analysis based on the fwhm of (311) peaks indicates that the average size of embedded spinel crystallites increases from 12 nm at 350 °C to 35 nm at 800 °C. Average crystallite sizes derived for other studied samples are also listed in Table 2 for a further comparison. It is important to note that the spinel crystallites produced from the embedded HT are about half the size of those derived from the pure-phase HT (31−

(17) Zeng, H. C.; Shi, S. *J. Non-Cryst. Solids* **1995**, *185*, 31.
(18) Chuang, C. C.; Wu, W. C.; Huang, M. C.; Huang, I. C.; Lin, J. L. *J. Catal.* **1999**, *185*, 423.
(19) Ji, L.; Lin, J.; Zeng, H. C. *J. Phys. Chem. B* **2000**, *104*, 1783.
(20) Powder Diffraction Files, γ-Al_2O_3 (no. 01-1308, no. 10-0425), Co_3O_4 (no. 09-418), $CoAl_2O_4$ (no. 44−0160), Joint Committee on Powder Diffraction Standards, Swarthmore, PA, 1995.

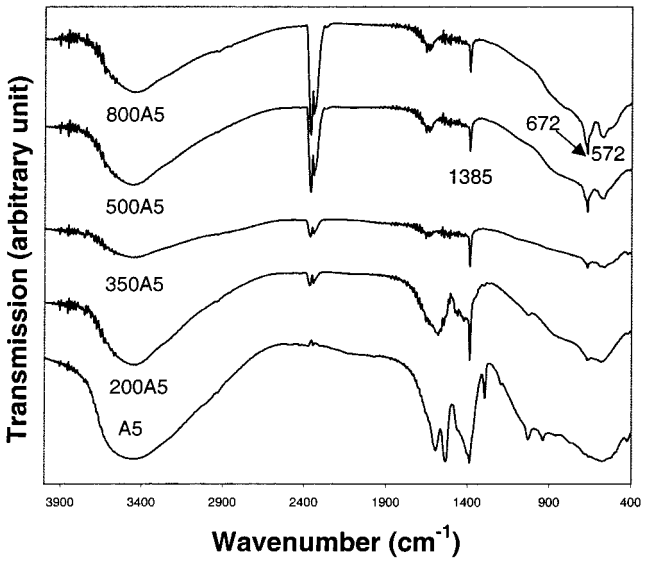

Figure 5. FTIR spectra of the HT-included biphasic gel sample A5 heated at different temperatures. The prefix number of the samples indicates the heating temperature (°C) (in static air, 4 h).

38 nm vs 62 nm at 800 °C). The retardation effect of the γ-Al_2O_3 matrix on the growth of the secondary phase (i.e., spinel nanoparticles) is thus evidenced in this work.

The FTIR investigation for depletion of organic inclusions in the biphasic precursors is reported in Figure 5. The majority of the organics (1900−900 cm^{-1}) can be readily removed when the biphasic samples are calcined at 200−350 °C. In the 1000−400 cm^{-1} region, typical stretching vibrations of Al−O and Co−O bonds in the spinel phase emerge,[6,11,21] which will be further discussed shortly. However, without including the HT compound, only part of the chelating organics can be decomposed at 300 °C,[13] because the acac−Al absorption features are still retained in heated blank alumina gels. Therefore, the presence of cobalt ions is responsible for the early decomposition of the organics in the gel matrixes. At 350 °C or higher, all organic groups are completely removed and spinel-phase absorptions become clearer in the 672−572 cm^{-1} region. The hydroxyl groups at 3500−3400 cm^{-1} can be attributed to uncondensed O−H groups in the original gel matrixes (e.g., A5 and 200A5), O−H groups of surface-hydrated oxides (which will be further addressed in the XPS investigation later), and O−H groups of the adsorbed water, noting that these bands are indeed proportional to the content of water in the high-temperature-treated samples (e.g., 350A5 to 800A5).

Thermal Evolution Processes. As reported above, the $Co^{II}Co^{III}_{2-x}Al_xO_4$−$Al_2O_3$ nanocomposites can be prepared by heating the biphasic gels at different temperatures for a certain period of time. In this subsection, we will investigate dynamical thermal processes during the generation of the nanocomposites using DSC/TGA methods. In particular, DSC scans for the pure-phase HT sample, blank alumina xerogel, and biphasic gel samples have been conducted in oxidative and nonoxidative atmospheres.

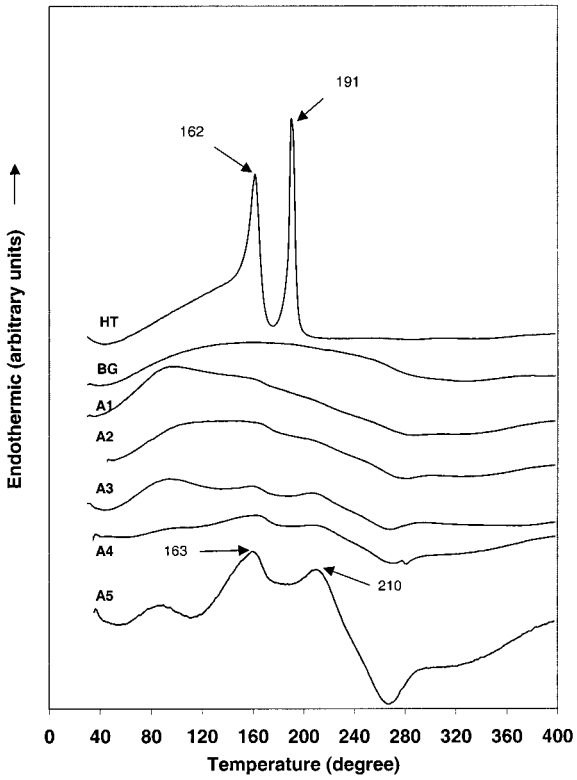

Figure 6. DSC curves of the alumina BG, the hydrotalcite-like compound HT, and the HT-included biphasic gel samples A1−A5 in a nitrogen stream.

For the pure-phase HT sample heated in nitrogen, as displayed in Figure 6, the first endothermic band below 162 °C is attributed to depletions of surface-adsorbed and interlayer water and the second large sharp peak at 191 °C to dehydroxylation of the hydrotalcite-like structure.[22,23] For the alumina blank gel (BG), the broad endothermic band over 40−320 °C can be assigned to the depletion of trapped water and PrOH that were produced as byproducts of the gelation reactions, which will be further studied using the TGA method. In the biphasic samples A1−A5, the small endothermic bands at 40−120 °C can be assigned to the depletion of trapped water and PrOH as in the case of the BG. The thermal events observed in the pure-phase HT and blank alumina gel can all be observed, except the intensities of the two large endothermic peaks at 162 and 191 °C have been significantly lowered. Furthermore, the peak positions have been slightly shifted to higher temperatures due to the confinement of the alumina matrix.

With an oxygen stream, as shown in Figure 7, extra redox reactions between the solid samples and gaseous oxygen molecules take place. For example, the higher temperature endothermic peak at 191 °C of the HT sample observed in a nitrogen atmosphere is no longer observed, which indicates that the two thermal events have been merged into one at 146 °C under a pure oxygen atmosphere. In the DSC scans for A1−A5, the first exothermic effects at about 200 °C are assigned to oxidation of the trapped organics such as the acac chelating reagent (refer also to Figure 5 for FTIR

(21) Gadsden, J. A. *Infrared spectra of minerals and related inorganic compounds*; Butterworths: London, 1975; p 43.

(22) Pesic, L.; Salipurovic, S.; Markovic, V.; Vucelic, D.; Kagunya, W.; Jones, W. *J. Mater. Chem.* **1992**, *2*, 1069.

(23) Xu, Z. P.; Zeng, H. C. *J. Mater. Chem.* **1998**, *8*, 2499.

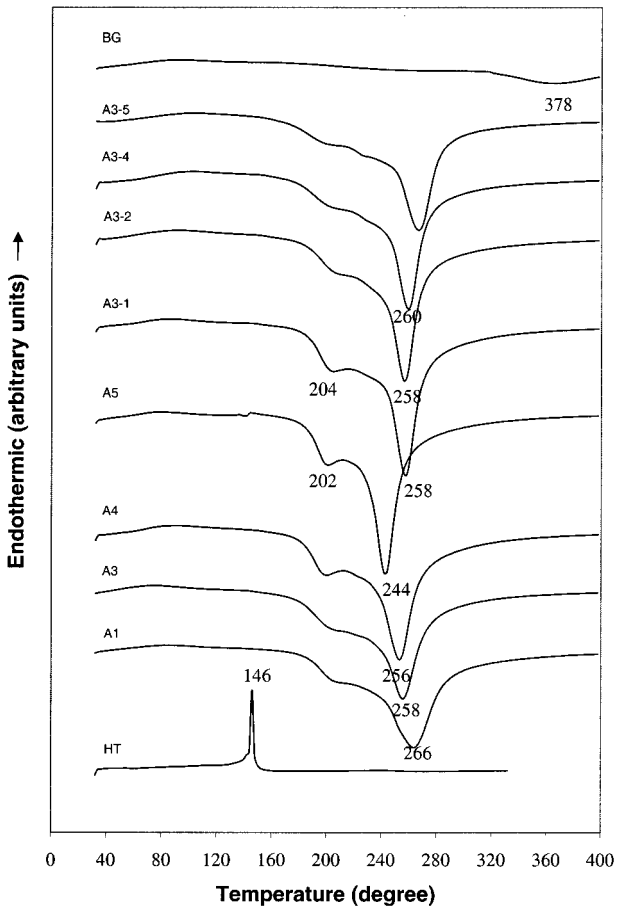

Figure 7. DSC curves of the alumina BG, the hydrotalcite-like compound HT, and the HT-included biphasic gels A1–A5 and A3-1 to A3-5 in an oxygen stream.

results, A5 vs 200A5). At higher temperatures, there are other exothermic events occurring at 244–266 °C. On the basis of the FTIR results (e.g., 200A5 vs 350A5), these bands should be attributed to combustion reactions between the retained organics (i.e., more tightly bonded acac groups in $Al(O\text{-}s\text{-}Bu)_{3-n}(acac)_n$) and gaseous oxygen.[13,24] It is interesting to note that, with an increase in HT content in the gels, the second exothermic bands are shifted toward lower combustion temperatures. This observation can be related to the catalytic effect of cobalt on hydrocarbon combustion.[24] Without HT inclusion, in fact, this combustion reaction has to be postponed to a much later stage in the blank-gel sample (378 °C). To explore the role of alumina matrixes during the biphasic gel reactions with oxygen gas, samples A3-1 to A3-5 have been further prepared in this work by varying the molar ratio of H_2O to ASB (H_2O added 0.5–3.0 mL) in the synthesis, noting that this sample series has the same HT content as sample A3 (ASB and HT fixed at 10.9 and 1.73 mmol). It is found that with a higher H_2O/ASB ratio gelation takes place in a shorter time. Because the second exothermic events are moved to the higher temperature region when the H_2O/ASB ratio increases, it seems that a shorter gelation time will generate denser gel matrixes, which would reduce oxygen accessibility to the gel matrixes.

The above DSC assignments are further supported by our TGA study. As reported in Figure 8, the only endothermic effect observed at 146 °C (Figure 7) for the HT sample indeed corresponds to a significant weight loss in the TGA measurement. The two exothermic bands in A1–A5, on the other hand, are also accompanied by two major weight losses over the same temperature region. For the latter cases, the completion of the second-stage weight loss is indeed Co metal (i.e., the HT content) dependent.

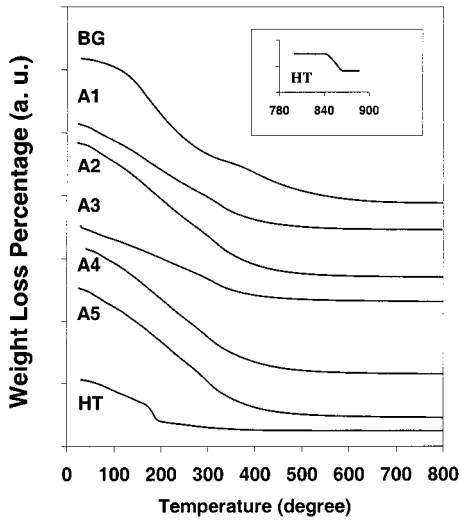

Figure 8. TGA weight losses of the alumina BG, the hydrotalcite-like compound HT, and the HT-included biphasic gel samples A1–A5 in an air stream.

Table 3. Specific Surface Areas, Total Pore Volume, and Average Pore Size for Some Calcined Samples at Selected Temperatures

sample	S_{BET}(350 °C[a]) ($m^2\,g^{-1}$)	S_{BET}(500 °C[a]) ($m^2\,g^{-1}$)	S_{BET}(800 °C[a]) ($m^2\,g^{-1}$)	TPV[b] ($cm^3\,g^{-1}$)	APV[c] (Å)
A1	326	270	224	0.38	44
A2	328	261	212	0.31	45
A3	363	269	201	0.34	41
A4	277	265	184	0.34	52
A5	304	253	195	0.32	49
A3-1	291	266		0.36	50
A3-2	304	258		0.39	49
A3-3	313	257		0.39	59
A3-4	326	253		0.42	52
A3-5	330	279		0.42	50
BG	684		234	0.34	
HT	53		6	0.15	

[a] Calcination temperature in static air (4 h). [b] Total pore volume for the samples calcined at 350 °C.[16a] [c] Average pore diameter for the samples calcined at 350 °C.[16a]

In Table 3, some of the textural properties of the calcined samples are listed for comparison. Unexceptionally, S_{BET} of the heated samples decreases with an increase in temperature. For example, for A1–A5 samples heated at various temperatures, S_{BET} is reduced gradually from 277–363 $m^2\,g^{-1}$ at 350 °C to 184–224 $m^2\,g^{-1}$ at 800 °C. It is interesting to note that the 350 °C heated blank alumina gel possesses a much higher S_{BET} (684 $m^2\,g^{-1}$, Table 3), compared to those of the biphasic gels heated at the same temperature. On the basis of the above DSC/FTIR/TGA results, it is understood that the Co-catalyzed combustions have largely been completed below 300 °C (Figures 5 and 7) whereas the same reactions for the non-cobalt-containing blank gel have to be carried out at a temperature higher than 350 °C. It is thought that the combustion heat released causes an early collapse of the amorphous

(24) Ji, L.; Lin, J.; Zeng, H. C. *Chem. Mater.* **2000**, *12*, 3466.

gel matrixes, which reduces the S_{BET} values of the samples. At higher calcination temperatures, sufficient thermal energy would iron out the difference created by the cobalt catalyst, which gives the essentially similar S_{BET} values for all the heated samples (e.g., 800 °C, Table 3). It should be mentioned that the total surface areas and other textural properties of these samples are contributed predominately by the alumina matrixes, because the related data of the pure-phase HT sample are much smaller after heating at the same temperatures (Table 3).

Spinel Phases in Nanocomposites. It has been known that the pure HT sample decomposes in an oxidative atmosphere at around 146 °C (Figure 7) and the majority of the weight loss of this compound is completed below 200 °C (Figure 8). In the confined state, the hydrotalcite-like structure is also destroyed at a temperature below 200 °C (Figure 4). Interestingly, due to this thermal decomposition, the cubic spinel structure (e.g., a small (311) peak) starts to form in the amorphous gel at a temperature as low as 200 °C. Nonetheless, the endothermic effect observed in the HT sample is not observable in the DSC curves of A1−A5 in Figure 7, which should be attributed to a smaller amount of the HT sample and a gradual thermal process in the biphasic gel matrixes. At higher calcination conditions, trapped organics decompose catalytically, and amorphous alumina gels turn to γ-Al_2O_3. Inevitably, the interdiffusion between the initially formed Co_3O_4 and alumina matrixes takes place, which will then generate $Co^{II}Co^{III}_{2-x}Al_xO_4$ ($0 \leq x < 1.63$) with the same crystallographic structure.[20]

Since the above two spinel phases cannot be efficiently resolved by XRD, we will use XPS, together with FTIR and TGA, to differentiate them in this subsection. Figure 9 shows some representative XPS spectra of O 1s.[25] The first peaks of the O 1s spectra, which are in the range of 529.6−530.1 eV, can be assigned to the surface oxygen (or oxygen of hydroxyl) in the Co spinel phases (or in the HT). The second peaks of the O 1s spectra (over 530.2−531.2 eV), on the other hand, are only observed in the gel samples (blank gel and A1−A5 biphasic gels). They are assigned to the surface oxygen in the alumina matrixes, because they cannot be observed in the heated HT sample. The third peaks of the O 1s spectra, which are observed in the range of 531.3−532.4 eV, are ascribed to the oxygen atoms in the surface hydroxyl groups, trapped nitrate ions, or adsorbed carbonates. The fourth peaks of the O 1s spectra, which are found in all samples, can be assigned unambiguously to the oxygen in surface water adsorbed, noting that the BEs = 532.2−534.0 eV measured for these peaks agree well with the literature data.[25]

In addition to the above O 1s data, the representative XPS spectra of the two metal cations Co 2p and Al 2p[25] of the nanocomposites are reported in Figure 10, and their BEs are listed in Tables 4 and 5, respectively. For the hydrotalcite-like phase (060A5), the large peak of Co $2p_{3/2}$ together with the second peak are assigned, respectively, to cobalt ions in octahedral sites formed by six hydroxyl groups in the HT compound and to anion-adsorbed surface cobalt during the compound synthesis or postsynthesis atmospheric adsorption of

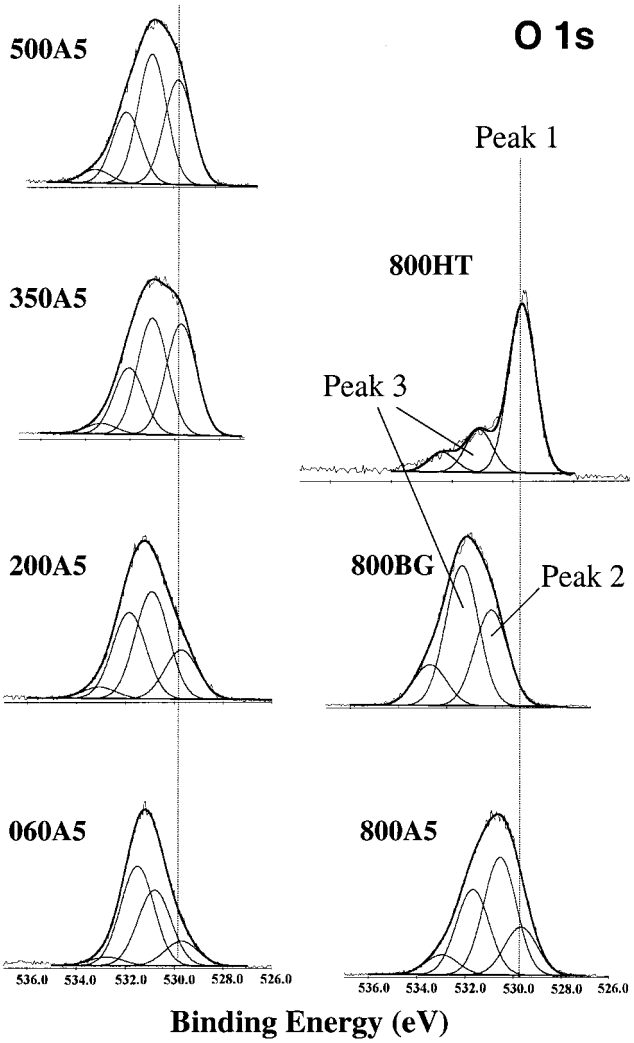

Figure 9. O 1s XPS spectra of the alumina BG, the hydrotalcite-like compound HT, and the HT-included biphasic gel sample A5 heated at different temperatures. The prefix number of the samples indicates the heating temperature (°C) (in static air, 4 h).

carbon dioxide.[26] For the 200 °C heated A5 (200A5), peaks 1 and 2 are almost identical to those of 060A5, which indicates that the local chemical environments of cobalt in the two samples are basically unaltered, although the HT phase has been decomposed at this temperature (Figure 4). Furthermore, it is noted that the intensities of the shake-up satellite peak (peak 3) of peak 1 in the two samples are about the same, which suggests that the population of divalent cobalt is not changed much upon the thermal treatment at 200 °C; i.e., the oxidation of divalent cobalt has just started. When the temperature increases to 350 °C, both BEs of peaks 1 and 2 of the 350A5 sample have values similar to those of the pure-phase Co_3O_4 (779.9 and 782.7 eV for the 800HT sample).[19,24,25] In addition to the common BE values observed, the intensities of the shake-up satellite peaks in the samples of 350A5 and 800HT are also similarly lower than those of 060A5 and

(25) Moulder, J. F.; Stickle, W. F.; Sobol, P. E.; Bomben, K. D. In *Handbook of X-ray photoelectron spectroscopy: a reference book of standard spectra for identification and interpretation of XPS data*; Chastain, J., Ed.; Physical Electronics Division, Perkin-Elmer Corp.: Eden Prairie, MN, 1992 (imprint).

(26) Xu, R.; Zeng, H. C. *Chem. Mater.* **2001**, *13*, 297.

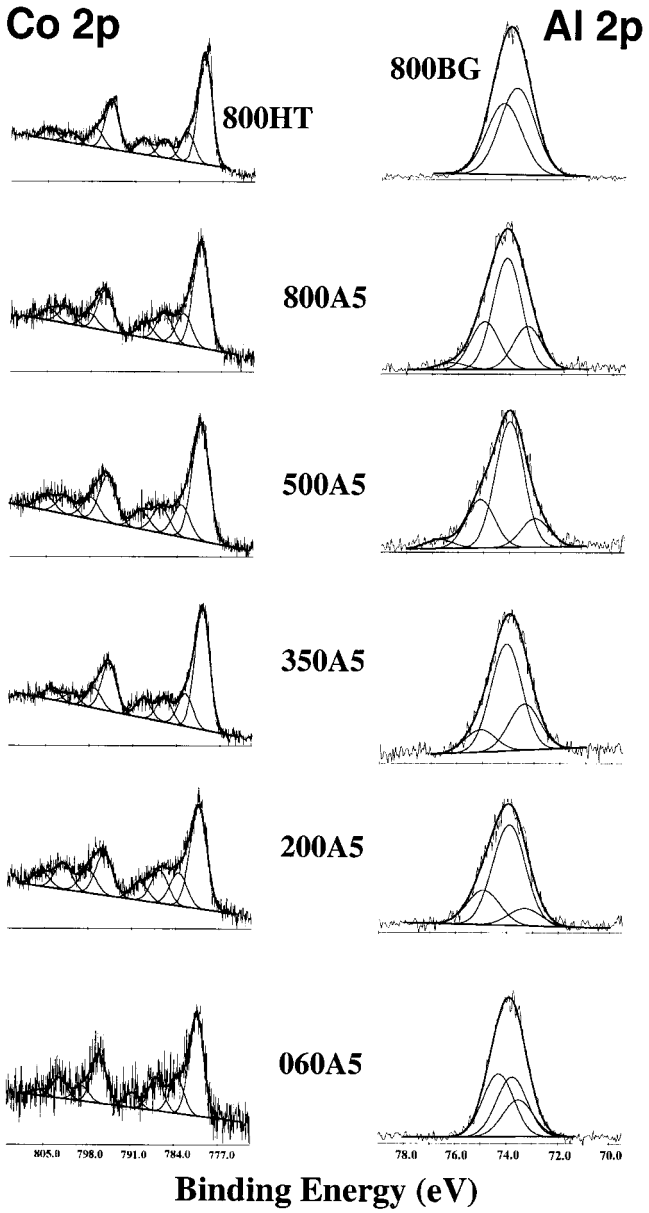

Figure 10. Co 2p and Al 2p XPS spectra of the alumina BG, the hydrotalcite-like compound HT, and the HT-included biphasic gel sample A5 heated at different temperatures. The prefix number of the samples indicates the heating temperature (°C) (in static air, 4 h).

200A5. The intensity lowering observed reveals an increase in trivalent cobalt, or an occurrence of divalent cobalt oxidation. Therefore, the spinel phase in 350A5 is a pure-phase Co_3O_4. With a further increase in temperature to 500 and 800 °C, the BEs of 500A5 and 800A5 increase slightly while the shake-up satellite peak intensities rise. These two changes indicate that there is a replacement of Co^{3+} in the spinel phase with Al^{3+} from the gel matrixes, because the BE of $Co^{II}Co^{III}_{2-x}Al_xO_4$ is higher than that of Co_3O_4 and the shake-up satellite is proportional to the divalent cobalt population in the spinel phase.[19,24,25] Indeed, this replacement of trivalent aluminum is a function of temperature. The replacement in 500A5 is small (i.e., x is small), which gives a spin–orbit splitting of 14.9 eV identical to that in the pure-phase Co_3O_4, whereas other $Co^{II}Co^{III}_{2-x}Al_xO_4$ spinels all have a value greater than 15.1 eV.[19,24,25] Similar observations can be obtained from

Table 4. Binding Energies (eV) of Co $2p_{3/2}$ of Two Surface Components for Some Calcined Samples at Selected Temperatures

sample[a]	peak 1[b]	peak 2[c]	SS[d] (eV)	spin–orbit splitting[e] (eV)	phase assignment
060A5	780.4	783.5	6.5	15.7	HT
200A5	780.3	783.5	6.2	15.1	HT (decomposed)
350A5	779.9	782.6	6.1	14.9	Co_3O_4
500A5	780.2	783.2	6.3	14.9	$Co^{II}Co^{III}_{2-x}Al_xO_4$
800A5	780.4	783.1	5.8	15.4	$Co^{II}Co^{III}_{2-x}Al_xO_4$
800HT	779.9	782.7	6.4	14.9	Co_3O_4
800A1	780.5	783.1	5.4	15.6	$Co^{II}Co^{III}_{2-x}Al_xO_4$
800A2	780.6	783.0	5.2	15.1	$Co^{II}Co^{III}_{2-x}Al_xO_4$
800A3	780.2	783.4	5.8	15.3	$Co^{II}Co^{III}_{2-x}Al_xO_4$
800A4	780.7	783.4	5.9	15.2	$Co^{II}Co^{III}_{2-x}Al_xO_4$
800A5	780.4	783.1	5.8	15.4	$Co^{II}Co^{III}_{2-x}Al_xO_4$

[a] The prefix number in each sample indicates the heat-treatment temperature (°C) (see the Experimental Section). [b] Peak 1 is assigned to Co cations in the hydrotalcite-like compound HT, or in spinels of Co_3O_4 and $Co^{II}Co^{III}_{2-x}Al_xO_4$ ($0 < x < 1.63$). [c] Peak 2 is attributed to Co bound directly to anion groups ($AO_3 = NO_3^-$ and/or CO_3^{2-}). [d] SS is the BE difference between the shake-up satellite peak 3 and peak 1. [e] Spin–orbit splitting between Co $2p_{3/2}$ and Co $2p_{1/2}$.

Table 5. Binding Energies (eV) of Al 2p for Some Calcined Samples at Selected Temperatures

sample[a]	Al–O–Co[b]	Al_2O_3[c]	$Al(OH)_n$[d]	$Al–AO_3$[e]
060A5	73.5	73.9	74.4	
200A5	73.3	73.9	74.9	
350A5	73.4	74.1	75.1	
500A5	73.0	74.0	75.1	76.7
800A5	73.3	74.1	74.9	76.2
800BG		73.8	74.3	
800A1	72.9	73.7	74.3	75.7
800A2	73.5	74.1	74.5	75.4
800A3	73.2	74.0	74.7	76.0
800A4	73.3	74.0	74.9	75.9
800A5	73.3	74.1	74.9	76.2

[a] The prefix number in each sample indicates the heat-treatment temperature (°C) (see the Experimental Section). [b] Al in connection with Co via an oxo bridge or a hydroxyl group. [c] Al in amorphous Al_2O_3 or γ-Al_2O_3 matrixes. [d] Al with hydroxyl groups (hydrated Al). [e] Al bound directly to anion groups (adsorbed $AO_3 = NO_3^-$ and/or CO_3^{2-}).

the analysis of the Al 2p spectra, as reported in Figure 10 and Table 5. The first Al 2p peaks at 72.9–73.5 eV are assigned to the aluminum of the gel matrix in contact with the included HT particles (060A5 and 200A5), or Al–O–Co linkages in the $Co^{II}Co^{III}_{2-x}Al_xO_4$ phase when there are thermal diffusions at higher temperatures,[26] noting that this peak is absent when there is no cobalt in the sample (800BG). The second and third Al 2p peaks can be assigned to the aluminum of γ-Al_2O_3 and its hydrated forms. The last Al 2p peaks (75.4–76.7 eV) are attributed to aluminum cations in association with the surface-adsorbed nitrate and carbonate anions when the samples are heated at higher temperatures (≥500 °C; see also Figure 5).[25]

The formation of the $Co^{II}Co^{III}_{2-x}Al_xO_4$ phase has also been confirmed by the FTIR investigation shown in Figure 5. The modification of Co_3O_4 with Al^{3+} has caused certain IR band shifts. Two characteristic absorptions of the spinel phase in the high-temperature-heated samples are 572 and 672 cm^{-1} respectively, which clearly depart from 572 and 665 cm^{-1} of the Co_3O_4 phase derived from the HT sample.

The above XPS/FTIR analyses have been further supported by a TGA investigation over 800–900 °C. As

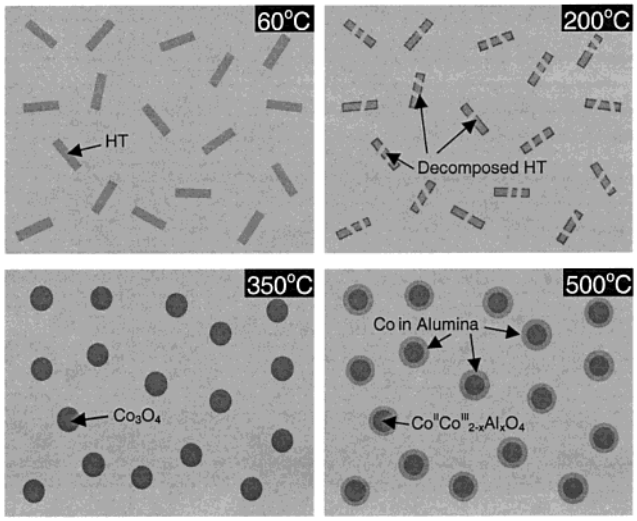

Figure 11. A schematic illustration of the main findings of this work: the included HT compound in an alumina matrix after drying, the decomposition of HT below 200 °C, the formation of the Co_3O_4 phase at 350 °C, and the conversion of Co_3O_4 to $Co^{II}Co^{III}_{2-x}Al_xO_4-Al_2O_3$ at higher temperatures (500−800 °C) due to interdiffusion between Co and Al.

reported in Figure 8, the TGA curve for the HT sample reveals a weight loss of 6.6% at 855 °C, which corresponds to the following chemical equilibrium:[27]

$$Co_3O_4 \rightleftarrows 3CoO + {}^1/_2O_2 \qquad (1)$$

However, a similar reaction does not occur in all biphasic gels (A1−A5), as no weight loss can be detected over the same temperature range (Figure 8) due to a lack of Co_3O_4. In agreement with the XPS assignments, pure-phase Co_3O_4 formed at low temperatures has been converted to the $Co^{II}Co^{III}_{2-x}Al_xO_4$ phase owing to the replacement of aluminum at higher temperatures. In view of the TGA results, all 800 °C heated samples can be assigned unambiguously to the $Co^{II}Co^{III}_{2-x}Al_xO_4$ phase, together with the XPS assignments listed in Table 4.

Figure 11 gives a schematic summary of the main findings in this work. One important issue that needs to be addressed in the future is the concentration gradient around a nanoparticle of $Co^{II}Co^{III}_{2-x}Al_xO_4$. As mentioned earlier, the formation of $Co^{II}Co^{III}_{2-x}Al_xO_4$ from Co_3O_4 indicates an interdiffusion between Co and Al. In this regard, $Co^{II}Co^{III}_{2-x}Al_xO_4$ particles should thus be enveloped with a layer of "Co-doped" alumina. Further investigations in this area will shed light on the fabrication of functional Co−Al gradient materials using the current method.

Conclusions

In summary, biphasic xerogels can be prepared by incorporation of the cobalt hydrotalcite-like compound $Co^{II}_{0.73}Co^{III}_{0.27}(OH)_{2.00}(NO_3)_{0.23}(CO_3)_{0.02}\cdot 0.5H_2O$ into Al_2O_3 matrixes during gel synthesis. When the above precursor gels are heated at different temperatures, cubic spinels of Co_3O_4 and $Co^{II}Co^{III}_{2-x}Al_xO_4$ can be sequentially generated in alumina matrixes with a static air atmosphere, which leads to formation of nanocomposites $Co^{II}Co^{III}_{2-x}Al_xO_4-Al_2O_3$ ($x \geq 0$). The average crystallite size of the embedded spinels increases from 9−13 nm at 350 °C to 31−38 nm at 800 °C, which is about half the size of that derived from the pure-phase cobalt hydrotalcite-like compound. The retardation effect of γ-Al_2O_3 matrixes on the growth of the spinel is thus evidenced. During the formation of the nanocomposites, the presence of cobalt ions is responsible for the early catalytic decomposition of the organics in the gel matrixes. Using different H_2O/ASB ratios in the gel synthesis, it has been found that a shorter gelation time generates denser gel matrixes, which would reduce oxygen accessibility to the gel matrixes. For the biphasic gels studied, S_{BET} is reduced gradually from 277−363 $m^2\ g^{-1}$ at 350 °C to 184−224 $m^2\ g^{-1}$ at 800 °C. The $Co^{II}Co^{III}_{2-x}Al_xO_4$ phase is developed with heating. On the basis of XRD/XPS/FTIR/TGA analysis, it is confirmed that Co_3O_4 starts to form at a temperature as low as 200 °C, and the pure-phase embedded Co_3O_4 can be obtained at 350 °C. At higher temperatures, 500−800 °C, the $Co^{II}Co^{III}_{2-x}Al_xO_4$ phase is formed with an increase in x due to the interdiffusion between the trivalent cobalt of Co_3O_4 and aluminum of the Al_2O_3 matrixes.

Acknowledgment. We gratefully acknowledge research funding (Grants R-279-000-064-112 and A/C50384) cosupported by the Ministry of Education and the National Science and Technology Board of Singapore.

CM010553O

(27) Oku, M.; Sata, Y. *Appl. Surf. Sci.* **1992**, *55*, 37.